Available at
www.ComputerScienceWeb.com
POWERED BY SCIENCE DIRECT®

ELSEVIER

Signal Processing 83 (2003) 11–29

SIGNAL PROCESSING

www.elsevier.com/locate/sigpro

Review

Digital equalisation in adaptive spatial filtering for radar systems: a survey

A. Farina*

Systems Analysis Group, Radar & Technology Division, Alenia Marconi Systems, Via Tiburtina Km. 12.400, 00131 Rome, Italy

Received 12 November 2001; received in revised form 30 April 2002

Abstract

In adaptive phased-array radar the cancellation of directional interference is limited by a number of mismatching sources; the main one is the frequency-dependent amplitude and phase mismatches between the radar receiving channels. A digital equalisation filter is needed to compensate for these mismatches. In this survey paper we describe the theory and practice of digital equaliser. We also demonstrate that the sampling rate of the analogue to digital converter has to be high enough to avoid the negative effects of folding of the interference spectrum after sampling. Several performance curves characterise the digital equaliser in terms of sampling rate and number of taps for different types of mismatches between the radar receiving channels. These curves are used to design the digital equaliser.

Keywords: Radar; Phased-array radar; Adaptive signal processing; Adaptive spatial filtering; Adaptive rejection of directional interference; Digital equaliser

1. Introduction

Electro magnetic (e.m.) noise like interference (NLI) disturb the correct working of radar by injecting noise from specific angular directions. Modern phased-array radar contrast this phenomenon via adaptive spatial filtering of the interference. This objective is reached by distorting the receiving antenna pattern by generating a null in the interference direction of arrival (IDoA). The technical procedure of spatial filtering is described in papers and text books (see, for instance [2]).

Adequate cancellation of the directional interference is obtained if the receiving channels are properly matched in amplitude and phase across the radar receiving bandwidth. This condition is necessary to attribute the amplitude and phase differences measured by the channels only to the nature (power and direction of arrival) of the impinging interference. Several are the mismatching sources; the imperfect matching of the analogue receiving channels is one of the main limitation to the interference cancellation. The effect of this mismatch on the interference cancellation ratio (ICR) has been studied in the literature; see [1–7]. A remedy to compensate for the mismatch is based on the use of an adaptive digital filter for equalisation (referred, in the following, as the digital equaliser); see [1,2,4–6]. The equalisation of receiving channels is important also

* Tel.: +39-06-4150-2279; fax: +39-06-4150-2665.
E-mail address: afarina@amsjv.it (A. Farina).

0165-1684/03/$ - see front matter
PII: S0165-1684(02)00389-4

Nomenclature

a	normalised sampling time of ADC devices
a_n, b	normalised amplitude and phase mismatches
B	radar receiver bandwidth
c	speed of light
d	distance between the phase centres of the main and auxiliary antennas
f	frequency
$G_M(\theta), G_A(\theta)$	one-way antenna gains of the main and auxiliary antennas
$H_{DE}(\omega)H_{ID}(\omega)$	transfer functions of a generic and of the ideal digital equalisers
$H_M(f), H_A(f)$	transfer functions of the main and auxiliary channels
ICR	interference cancellation ratio
ICR_{DE}, ICR_{NDE}	interference cancellation ratios in presence and in absence of digital equaliser
INR	interference to noise power ratio
L	number of taps of the digital equaliser
M	order of the Butterworth filters
N	number of auxiliary channels
$p_i, i = 1, \ldots, M$	poles of the Butterworth filters
T	time duration of a delay of the digital equaliser
λ_0	wave length
θ	angular co-ordinate measured with respect to the normal to the antenna array face
ω	normalised angular pulsation
w	adaptive weight
$\mathbf{w}$	weight vector of the digital equaliser

Acronyms

ADC	analogue to digital converter
e.m.	electromagnetic
FIR	finite impulse response
IDoA	interference direction of arrival
IF	intermediate frequency
I,Q	in-phase and quadrature signal components
NLI	noise like interference
NST	normalised sampling time
PRNS	pseudo-random noise sequence
RX	analogue receivers
STAP	space–time adaptive processing

for space–time adaptive processing (STAP) for airborne radar application; the problem of channel equalisation for these systems was mentioned in [8, p. 186].

This survey paper offers a comprehensive and unified view of the topic through the collection of the following contributions:

- cancellation performance due to imperfect channel matching,
- basic principles of the digital equaliser applied to adaptive phased-array radar,
- details of how the digital equaliser should be implemented in practice,
- recovery of cancellation performance in presence of digital equaliser for several cases of practical interest,
- guidelines to select the following system parameters:

(i) proper sampling rate of signals in the analogue to digital converter (ADC),
(ii) number of taps of the digital equaliser,
(iii) shape, power and number of samples of the calibration sequence of the digital equaliser.

These points seem not adequately covered in the technical literature, a noticeable exception being the paper by K. Gerlach [4] in which items (ii) and (iii) are tackled. This analysis is of interest also for the other systems, such as sonar, communication and radio astronomy, where the adaptivity plays a role. The importance of such survey for both practitioners and researchers in adaptive array processing seems evident.

The remaining part of the paper is organised as follows. Section 2 introduces the key equations to evaluate the deleterious effects of the aforementioned receiving channel mismatch on ICR. The working principle of the digital equaliser for adaptive phased-array radar is illustrated in Section 3. Section 4 presents a detailed analysis concerning the application of the digital equaliser. It is shown that the signal sampling rate plays a major role; guidelines for the selection of the sampling rate and the number of equaliser taps are given. Concluding remarks are in Section 5. Some mathematical details are in the appendices.

A note on the symbols. Vectors and matrices are represented with lower and upper case bold letters, respectively. The superscripts: $(\bullet)^*, (\bullet)^{\mathrm{T}}, (\bullet)^{\mathrm{H}}$ stand for complex conjugate, transpose and Hermitian (i.e.: complex conjugate and transpose) operations. For sake of convenience, the variables f (the frequency) and ω (the angular pulsation) are freely interchanged without rising confusion.

2. Mismatch of the receiving channels

A first cut analysis of the effect of the amplitude and phase mismatching of analogue radar receiving channels is as follows. Consider the simple system equipped with the main and one auxiliary channels. Assume sinusoidal ripples vs. frequency f for the transfer functions of the main and auxiliary channels in the receiving band

$$H_{\mathrm{M}}(f) = 1 + \varepsilon_p \sin(\theta_{\mathrm{M}} + 2\pi f/f_{\mathrm{M}}), \qquad H_{\mathrm{A}}(f) = 1 + \varepsilon_p \sin(\theta_{\mathrm{A}} + 2\pi f/f_{\mathrm{A}}), \tag{1}$$

where ε_p is the amplitude of the sinusoidal ripples, θ_{M} and θ_{A} are unknown quantities modelled as independent random variables, uniformly distributed over $[0, 2\pi]$; the respective ripple frequencies are f_{M} and f_{A}. The sinusoidal ripples account for the signal reflections produced by impedance mismatch at both ends of the filters in the receiving channels. This model has been verified experimentally (see [1, p. 305]) and also hypothesised for calculations by researchers (see [2,3,5–7]). It can be shown that the ICR (see Appendix A), i.e.: the ratio of the input to output interference power values, after adaptive spatial filtering of the interference is $\mathrm{ICR} = 2\varepsilon_p^{-2}$; this means that very accurate matching is required to obtain good interference cancellation. For instance, to obtain 40 dB of ICR we need to specify $\varepsilon_p = 0.01\sqrt{2} = 0.014$, which is a very tight requirement. Expressing the ε_p in radians we obtain the required tolerance for the in band phase mismatch. For example, to have 40 dB of ICR, the tolerance should be 0.80°. For contemporary presence of amplitude and phase mismatches, the ICR has a more complex expression which is derived in Appendix A. By applying Eq. (A.5) with the numerical values: bandwidth of the receiving channels $B = 5$ MHz and interference-to-noise power ratio $\mathrm{INR} = 50$ dB, it is possible to depict in Fig. 1 the ICR contour curves versus the normalised amplitude $a_{\mathrm{n}} = a_{\mathrm{A}}/H_0$ and the phase mismatches b (degrees) (see Appendix A for the precise definition of these parameters).

It is seen that to have 40 dB of ICR, we need to specify tight requirements for both amplitude (below 1%) and phase (below 0.7°) mismatches. This figure motivates the need to resort to equalisation filters in the radar digital section to compensate for the mismatches of the auxiliary channels (in their analogue part) with respect to the main channel. This is the subject of the next section.

3. Compensation of the receiver channel mismatch

Few methods have been devised to contrast the deleterious effects of unavoidable mismatches of analogue receivers. Figs. 2 and 3 illustrate the use of an adaptive digital finite impulse response (FIR) filter to equalise the amplitude and phase responses of the N auxiliary receivers $(\mathrm{RX}_1, \mathrm{RX}_2, \ldots, \mathrm{RX}_N)$ to those of the main receiver $(\mathrm{RX}_{\mathrm{M}})$. The FIR is made of L taps, T seconds far apart. The filter weights are determined to minimise the power of the difference signals between the main and each auxiliary channel outputs. The adaptive equaliser works in two phases. First phase (Fig. 2): calculation of the FIR weights by using a pseudo-random noise

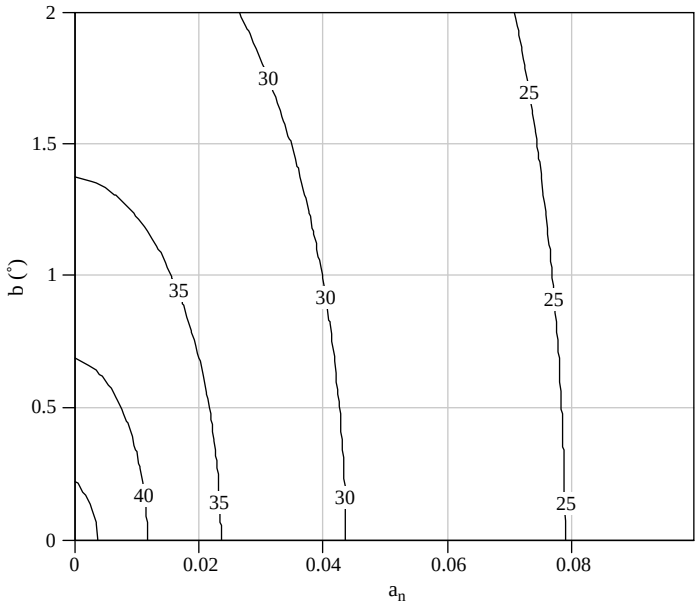

Fig. 1. Contour curve of ICR (dB) versus the amplitude (in natural number, along the horizontal axis) and phase (in degrees, along the vertical axis) mismatches of the analogue receiving channels.

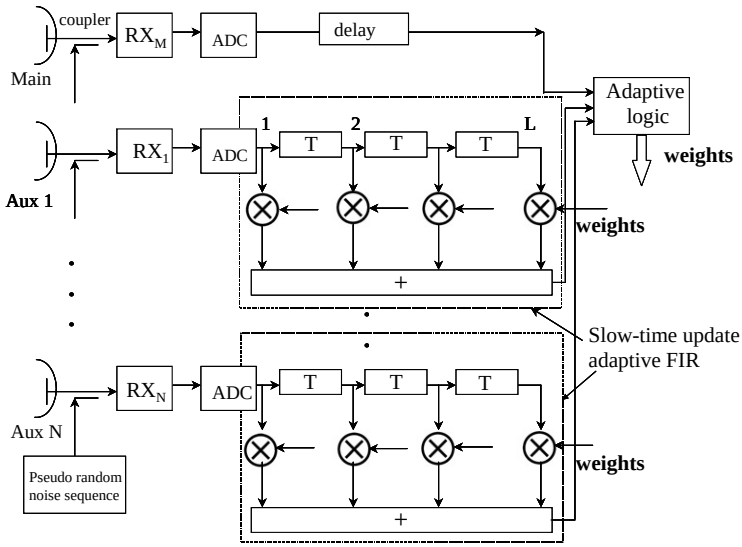

Fig. 2. Training (first phase) of the adaptive equalisers.

sequence (PRNS) with flat spectrum that occupies the whole frequency band—including the tails—of the receivers. The PRNS is injected into the $N + 1$ radar channels via microwave coupler devices. Second step (Fig. 3): once the weights of the equalisation FIRs have been calculated, their values are frozen. The PRNS source is disconnected and the outputs of the main and of the equalised auxiliary channels are processed by the adaptive interference canceler that filters out the NLI by the main radar channel.

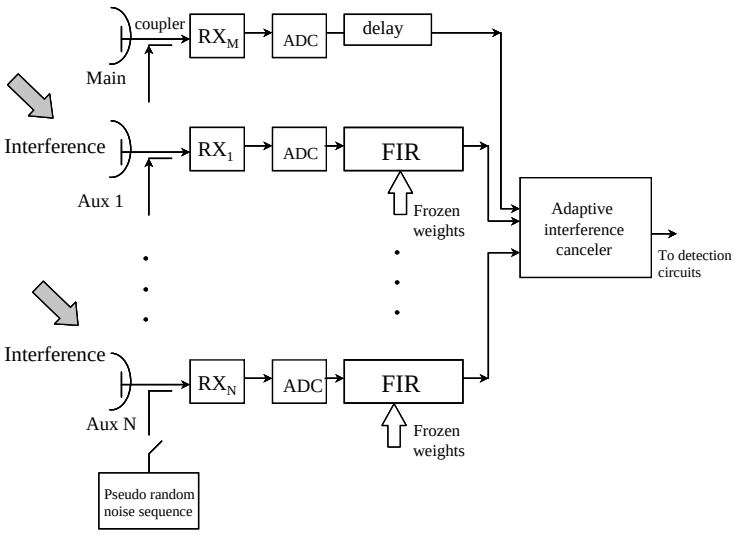

Fig. 3. Adaptive interference canceler applied to the equalised auxiliary channels (second phase).

Note that the weights of the equaliser are updated in accordance to the receiver component drifts due to ageing and environmental conditions; say, every several minutes. Instead, the weights of the adaptive interference canceler need to be updated every hundreds of μs depending on the rotation speed of the antenna which modulates the amplitude of the interference signal received by the radar. This weight update is related also to the temporal variation of the NLI source power. Thus, the amount of extra computational power, required to set the weights of the adaptive equaliser, is modest with respect to the computational power required for calculating the weights of the usual adaptive interference canceler. The real time application of the equalisation weights to the N sequences of auxiliary received samples needs fast pipelines of sum and multiply devices; this processing is, in general, computationally intensive.

To study in more detail the equalisation procedure, consider the simplified scheme of Fig. 4 which refers to the main and one auxiliary channels. This scheme has been analysed previously in [2–5]; here we recall the working principle and derive the main equations in view of the subsequent performance analysis of Section 4.

The calibration signal has power P_I and flat spectrum. The additive noise is white of power P_N; the noise processes are independent of each other. $H_M(f)$ and $H_A(f)$ represent the frequency responses of the analogue receivers of the main and auxiliary channels, respectively. The two ADCs sample and digitise the main and auxiliary signals. An equalisation FIR filter with L taps and L weights is present in the auxiliary channel. The equaliser properly combines the sequence of auxiliary signals $\mathbf{x}^T = [x_1\ x_2\ \ldots\ x_L]$ and subtracts the result from the main signal sample x_M; the output signal is v.

Ideally the equalisation filter should have the following transfer function:

$$H_{ID}(f) = \frac{H_M(f)}{H_A(f)}. \tag{2}$$

As a simple example consider the case of a triangular amplitude mismatch between the auxiliary and the main receivers. The filter transfer function of the equaliser has the amplitude response illustrated in Fig. 5; note that the inverse of portions of straight lines are hyperbolas; however, they still look as a straight lines—with opposite slopes—because of the small value of the amplitude mismatch. The intersections of $|H_A(f)|$ and $|H_{ID}(f)|$ with $|H_M(f)|$ occur at the same frequencies $\pm f^*$. Similar reasoning applies to the phase mismatch:

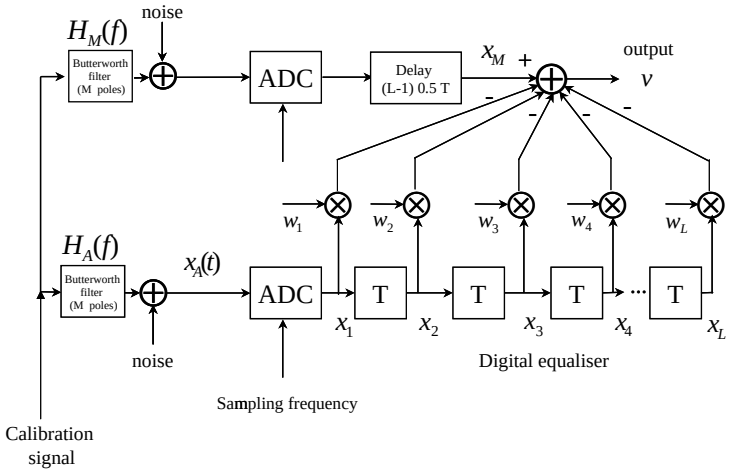

Fig. 4. Calculation of the weights of the equalisation filter.

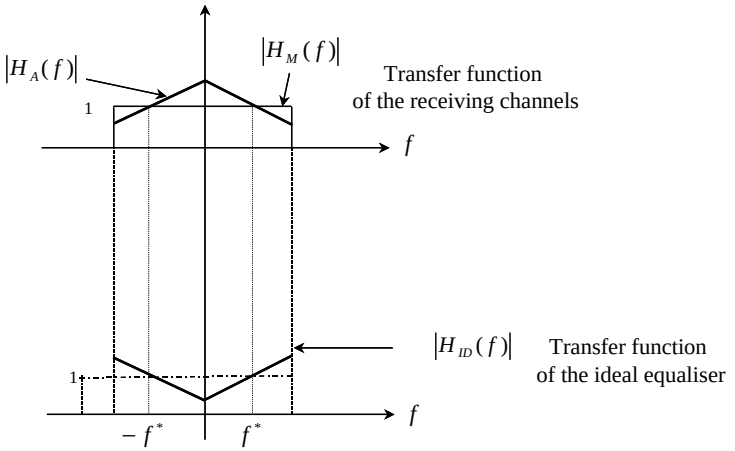

Fig. 5. Transfer function of an ideal equaliser; a triangular amplitude mismatch has been hypothesised.

the phase response of the ideal equalisation filter should be the difference between the phases of the main and of the auxiliary channels. Thus the response of the equaliser is required to be a very accurate reproduction of the receiver mismatch; this is possible with the digital technology.

In practice, the ideal equaliser can be approximated by a digital FIR filter having L taps, T seconds far apart. Fig. 4 illustrates the way in which the L-dimensional weight vector $\mathbf{w} = [w_1\ w_2 \ldots w_L]^{\mathrm{T}}$ of the digital equaliser is calculated. It is a conventional least-squares method, i.e. the weight vector $\mathbf{w}$ is found so that $E\{|v|^2\} = \min$. The weight vector

$$\mathbf{w} = \mathbf{R}^{-1}\mathbf{r} \tag{3}$$

is obtained by the classical Wiener filter expression (see, for instance, [2, p. 100, Eq. (4.5b)]). It requires the estimation and inversion of the covariance matrix

$$\mathbf{R} = E\{\mathbf{x}^*\mathbf{x}^{\mathrm{T}}\} \tag{4}$$

of the sequence $\mathbf{x}^{\mathrm{T}} = [x_1\ x_2\ \ldots\ x_L]$ to multiply to the estimated cross-correlation

$$\mathbf{r} = E\{\mathbf{x}^* x_{\mathrm{M}}\} \tag{5}$$

between $\mathbf{x}$ and x_{M}. The sample x_{M} is centred with respect to the sequence of auxiliary samples; this is achieved by the delay line $(L-1)0.5T$ (L is taken to have an odd value) which is shown in Fig. 4 along the main channel. Ideally, if $H_{\mathrm{M}}(f) = H_{\mathrm{A}}(f)$, the equalisation weight vector would be: $\mathbf{w} = [0\ 0\ 1\ 0\ 0]^{\mathrm{T}}$ for $L = 5$.

The receiver mismatch in the analogue sections of the receiving channels can be accurately compensated for in the digital sections provided that the signal spectra after the ADC are an accurate reproduction of the analogue spectra. This requires that the ADC sampling rate be high enough to reduce the aliasing of the spectrum tails. If the ADC sampling frequency is not properly selected, the digital equaliser will determine its weights on the basis of the folded spectra rather than the analogue spectra; this was originally noted in [4]. To give guidelines on the selection of the ADC sampling rate and on the number L of taps of the digital equaliser we need to select suitable expressions for the analogue receivers of the main and auxiliary channels.

Butterworth filters are selected to emulate the analogue radar receivers [4]. The transfer function of the Butterworth filter is

$$H(\omega) = \frac{\sqrt{(M/\pi)\sin \pi/2M}}{\prod_{i=1}^{M} (\mathrm{j}\omega - p_i)}, \tag{6}$$

where M is the order of the filter, p_i, $(i = 1, 2, \ldots, M)$ are the poles of the filter and ω is the angular pulsation.[1] The Butterworth filter has the poles on the unity circle equally spaced in angle

$$p_i = \mathrm{j}e^{\mathrm{j}(\pi/2M)(2i-1)}, \quad i = 1, 2, \ldots, M, \tag{7}$$

where $\mathrm{j} = \sqrt{-1}$. To have a stable filter $\mathrm{Re}(p_i) < 0$, $i = 1, 2, \ldots, M$; i.e.: the poles have to lie on the lhs half of the complex plane. The numerical values of the poles for $M = 1, 2, 3, 4$ and 8 are reported in Table 1

Table 1
Values of the poles of the ideal Butterworth filters, of order $M = 1$, 2, 3, 4 and 8, used in the main channel for several study cases

Filter order, M	Poles			
1	1st pole: −1			
2	1st pole: −0.7071067812 +0.7071067812j	2nd pole: −0.7071067812 −0.7071067812j		
3	1st pole: −0.5 + 0.8660254038j	2nd pole: −1	3rd pole: −0.5 − 0.8660254038j	
4	1st pole: −0.3826834324 +0.9238795325j	2nd pole: −0.9238795325 +0.3826834324j	3rd pole: −0.9238795325− 0.3826834324j	4th pole: −0.3826834324 −0.9238795325j
8	1st pole: −0.195090322 +0.9807852804j	2nd pole: −0.555570233 +0.8314696123j	3rd pole: −0.8314696123 +0.555570233j	4th pole: −0.9807852804 +0.195090322j
	5th pole: −0.9807852804 −0.195090322j	6th pole: −0.8314696123 −0.555570233j	7th pole: −0.555570233 −0.8314696123j	8th pole: −0.195090322 −0.9807852804j

[1] For convenience the analysis proceeds by using the angular pulsation ω; equations in the frequency domain f are straightforward.

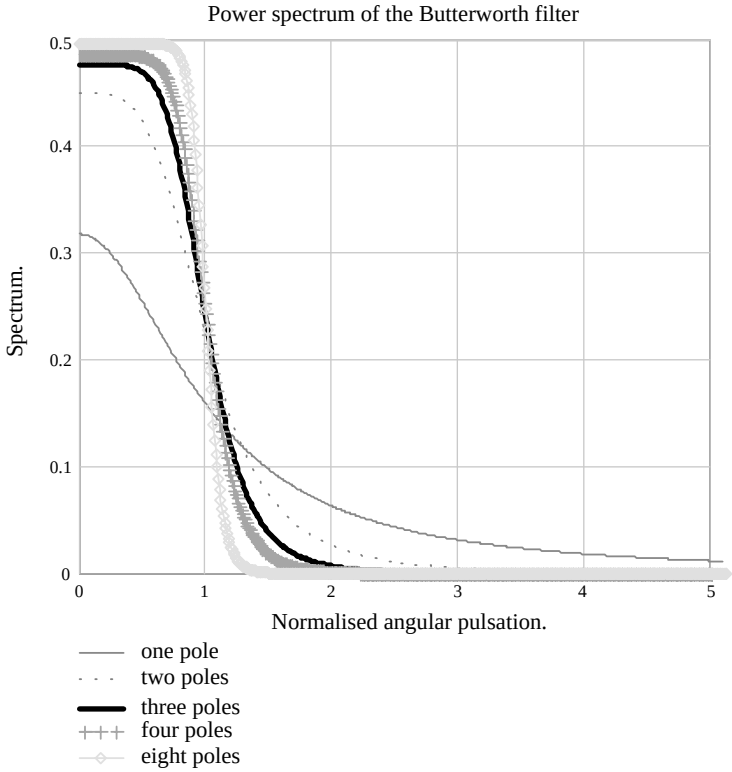

Fig. 6. Squared modulus of the transfer function of a Buttherworth filter of order M.

(see also Appendix B). The squared modulus of the filter is

$$|H(\omega)|^2 = \frac{(M/\pi)|\sin(\pi/2M)|}{1+\omega^{2M}}; \tag{8}$$

The numerator of (8) has been selected so that $\int_{-\infty}^{\infty} |H(\omega)|^2 \, d\omega = 1$. Fig. 6 depicts $|H(\omega)|^2$ for several values of the order M; it is noted that by increasing the filter order, the tail has a sharper decrease; in other words the skirts of the transfer function are directly influenced by the poles.

The horizontal axis of the figure shows $\omega/(\pi B)$; i.e.: the angular pulsation ω has been normalised to the desired angular half-bandwidth πB, being B the -3 dB filter band containing both negative and positive frequencies; this assumption will hold true for the remaining portion of the paper.

In [4] Gerlach performed a complex perturbation analysis, of the position of the filter poles, involving a lot of mathematics; here we prefer to proceed in a simpler yet effective manner. The mismatching of the auxiliary channel has been emulated by a slight arbitrary modification of the poles of ideal filter which has been taken to represent the main channel. This procedure has a physical base: in fact the ageing of the components changes the poles of the analogue filters. Table 2 (see also Appendix B) collects numerical values of the poles for the mismatched Butterworth filters; these have been selected—with a "try and see" procedure—to give ICR = 34.5 dB, in absence of digital equaliser, when the INR = 50 dB. Note that the best value of ICR one could obtain is 47 dB; the 3 dB that are missed to 50 dB are related to the summation of the thermal noise in the main and auxiliary channels. It is the aim of the next section to show in which conditions the digital equaliser is able to recover the 12.5 dB that are missed with respect to the ideal value of 47 dB.

Table 2
Values of the poles of the Butterworth filters, of order $M = 1$, 2, 3, 4 and 8, used in the receivers of the mismatched auxiliary channels

Filter order, M	Poles			
1	1st pole: -0.9645			
2	1st pole: $-0.737 - 0.707$j	2nd pole: $-0.707 + 0.707$j		
3	1st pole: $-0.5 + 0.86$j	2nd pole: -1	3rd pole: $-0.5 - 0.84675$j	
4	1st pole: $-0.380 + 0.9162$j	2nd pole: $-0.923 + 0.371$j	3rd pole: $-0.923 - 0.371$j	4th pole: $-0.382 - 0.9162$j
8	1st pole: $-0.194 + 0.979$j	2nd pole: $-0.554 + 0.830$j	3rd pole: $-0.831 + 0.543$j	4th pole: $-0.979 + 0.191$j
	5th pole: $-0.980 - 0.195$j	6th pole: $-0.831 - 0.535$j	7th pole: $-0.555 - 0.829$j	8th pole: $-0.196 - 0.981$j

Different sets of poles of the mismatched filters may give the same ICR; we selected the set in Table 2 to assess the benefit of the digital equaliser (see next section).

The interference cancellation ratio, without the presence of the digital equaliser, is (see [2, p. 101])

$$\mathrm{ICR}_{\mathrm{NDE}} = \frac{1}{1 - |\rho|^2}, \tag{9}$$

being the cross-correlation coefficient ρ, between the main and auxiliary signals, equal to

$$\rho = \frac{\int_{-\infty}^{\infty} H_{\mathrm{M}}(\omega) H_{\mathrm{A}}^{*}(\omega)\,\mathrm{d}\omega}{\sqrt{\int_{-\infty}^{\infty} |H_{\mathrm{A}}(\omega)|^2\,\mathrm{d}\omega + 1/\mathrm{INR}}\sqrt{\int_{-\infty}^{\infty} |H_{\mathrm{M}}(\omega)|^2\,\mathrm{d}\omega + 1/\mathrm{INR}}}, \tag{10}$$

where INR is the interference-to-noise power ratio.

The cross-correlation coefficient ρ is calculated by finding the mathematical expressions of the power and cross-power values of the signals in the two channels in the angular pulsation domain. In fact, in lieu of calculating the average in time of the product of two signals, we calculate the integration in the angular pulsation domain of their cross-power spectral density because we invoke the Wiener–Khintchine theorem.

In the numerical evaluation described in the next Section, INR has been taken equal to 50 dB. In the ideal case of $H_{\mathrm{M}}(\omega) = H_{\mathrm{A}}(\omega)$, the maximum cancellation value is

$$\mathrm{ICR}_{\max} = \frac{\mathrm{INR}}{2}. \tag{11}$$

In our case: $\mathrm{ICR}_{\max} = 47$ dB, as it was already pointed out.

The ADC sampling interval is taken as: $T = a/B$, when $a = 1$ the sampling period is $T = 1/B$ which is the Nyquist sampling period. In the numerical analysis of the next section, the parameter a is allowed to vary in the interval: [0,1]. The canceler behaviour is established as a function of the ADC sampling period. Call the parameter $a = T/1/B$ the normalised sampling time (NST) of the ADC; NST $= 0$ means infinitely high sampling frequency, i.e.: duration of delay of digital equaliser, $T = 0$; NST $= 1$, means ADC sampling frequency equal to the Nyquist sampling frequency.

Note that the digital equalisation filter replicates outside the interval $[-1/a, 1/a]$; thus, it is able to approximate the filter response of the ideal digital equaliser (2) only in this interval.

The mathematical expressions of the elements of $\mathbf{R}$ (Eq. (4)) and $\mathbf{r}$ (Eq. (5)) are

$$\begin{aligned} R_{nm} &= P_{\mathrm{I}} \int_{-\infty}^{\infty} |H_{\mathrm{A}}(\omega)|^2 \mathrm{e}^{\mathrm{j}\omega\pi BT(n-m)}\,\mathrm{d}\omega + \delta(n-m)\frac{1}{\mathrm{INR}}, \quad n,m = 1,2,\ldots,L, \\ r_{\mathrm{n}} &= P_{\mathrm{I}} \int_{-\infty}^{\infty} H_{\mathrm{A}}^{*}(\omega) H_{\mathrm{M}}(\omega) \mathrm{e}^{-\mathrm{j}\omega\pi BT[(L-n)-(L-1)/2]}\,\mathrm{d}\omega, \quad n = 1,2,\ldots,L, \end{aligned} \tag{12}$$

where

$$\delta(n-m)=\begin{cases}1 & \text{for } n=m,\\ 0 & \text{for } n\neq m.\end{cases}$$

is the Kronecker delta function. These expressions take also into account the delays along the main and auxiliary channels as depicted in Fig. 4. Note that the phase term in the first equation of (12) should be $\omega T(n-m)$; however, by introducing the normalised angular pulsation $\omega_n=\omega/(\pi B)$, the phase term $\omega T(n-m)$ is replaced by $\omega_n \pi BT(n-m)$; to avoid abuse of notation we write $\omega\pi BT(n-m)$. A similar reasoning applies also to the second equation of (12).

The interference cancellation in presence of the equalisation filter is (see Appendix C)

$$\mathrm{ICR}_{\mathrm{DE}}=\frac{1}{1-\mathbf{r}^{\mathrm{H}}\mathbf{R}^{-1}\mathbf{r}\mathrm{INR}/(\mathrm{INR}+1)}. \tag{13}$$

Note that Eq. (13) reduces to Eqs. (9) and (10) when: the number of taps of the digital equaliser is $L=1$, $P_l=1$, and $\int_{-\infty}^{\infty}|H_M(\omega)|^2\,\mathrm{d}\omega=1$. This statement is also clarified in Appendix C.

4. Performance analysis

In this section we collect a number of performance curves that illustrate the behaviour of the digital equaliser. The analysis refers to the scheme of Fig. 4. Purposely, the presence of the antennas and of the different propagation paths of the interference towards the two antenna phase centres have been excluded from the analysis to focus the attention just on the mismatch between the receiving channels.

In the following, Eq. (13) is calculated for several cases of practical interest:

- the analogue radar receiving channels are emulated with Butterworth filters having the following number of poles: $M=1,2,3,4$ and 8; the numerical values of poles of the main channel are those in Table 1; Table 2 provides the poles of the auxiliary channel; the -3 dB bandwidth of the filters is $B=5$ MHz;
- the NST a varies in [0,1]; the over-sampling (i.e.: $a<1$) is needed to avoid undesired aliasing effects of the calibration signal through the skirt of the filters $H_M(f)$ and $H_A(f)$ which might not have a very strong fall-off;
- the equalisation filter has L taps; in the numerical examples that follow L takes four values: 1 (i.e.: no digital equaliser), 3, 5 and 7;
- the calibration to noise power ratio is 50 dB.

Figs. 7–11 display the ICR(dB) vs. the normalised sampling time of the ADC. Four curves are shown in the figures: the straight line at the bottom corresponds to the absence of digital equaliser; the remaining three curves give the ICR when the number of taps of the digital equaliser are $M=3$, 5 and 7, respectively. The upper horizontal line of the figure is set at 47 dB which is the maximum achievable value of the ICR. The vertical distance between the line at 34.5 dB ($L=1$) and one of the three curves gives the ICR gain achieved by the digital equaliser having L taps and operating with a prescribed normalised sampling time a. The vertical distance between the line at 47 dB and one of the three curves gives the ICR gain still missed by the digital equaliser having L taps and operating with a prescribed normalised sampling time a. From Figs. 7–11 the number of poles of the Butterworth filters increases from 1 up to 8.

The following observations are in order:

1. The increase of the order of the Butterworth filters improves the ICR; this is attributable to the steeper fall off of the tails of the filter leading to less aliasing.

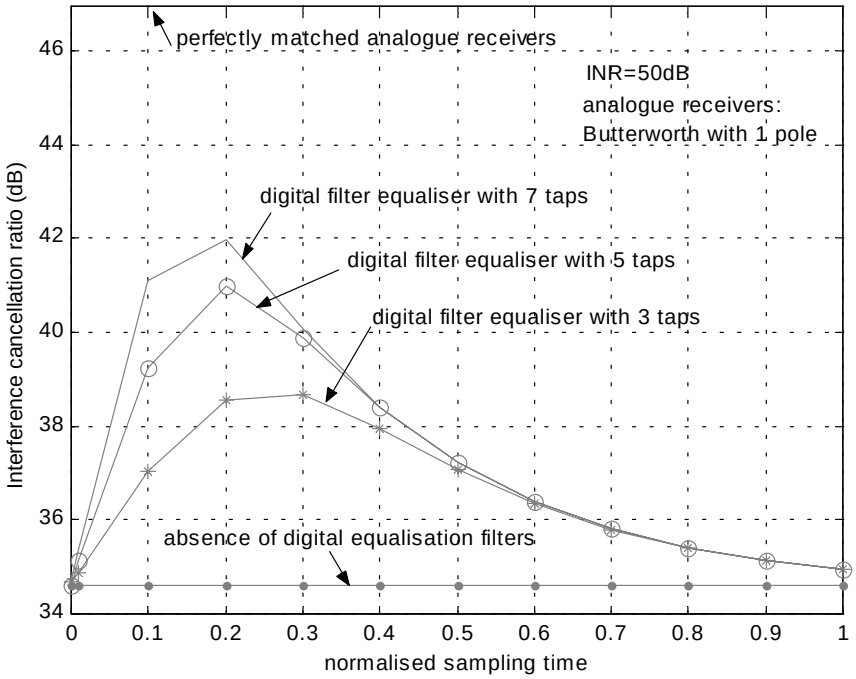

Fig. 7. ICR vs. the normalised sampling time. The analogue receivers are emulated with Butterworth filters having $M = 1$ pole; the digital equaliser has $L = 3$, 5 and 7 taps; INR = 50 dB.

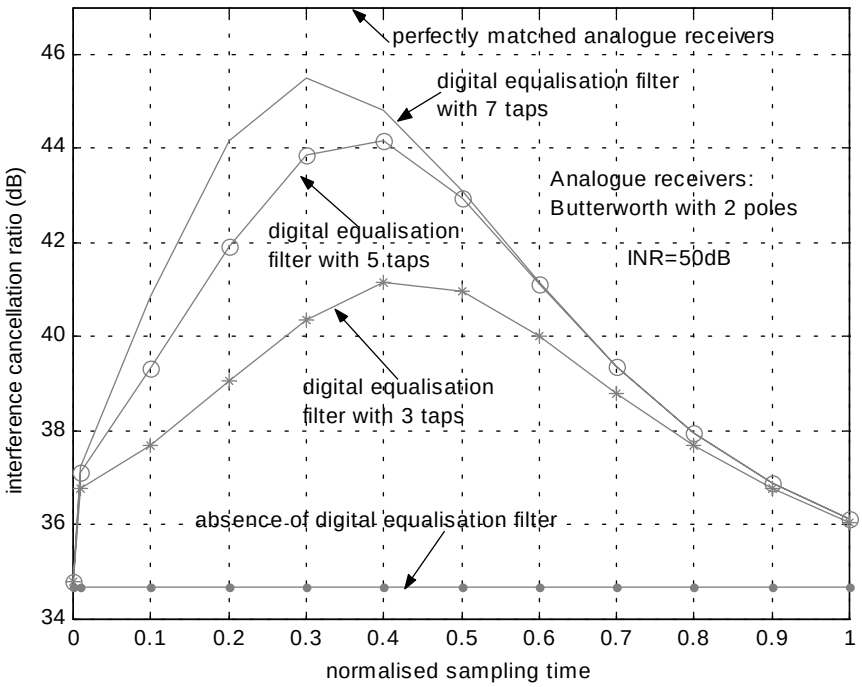

Fig. 8. ICR vs. the normalised sampling time. The analogue receivers are emulated with Butterworth filters having $M = 2$ poles; the digital equaliser has $L = 3$, 5 and 7 taps; INR = 50 dB.

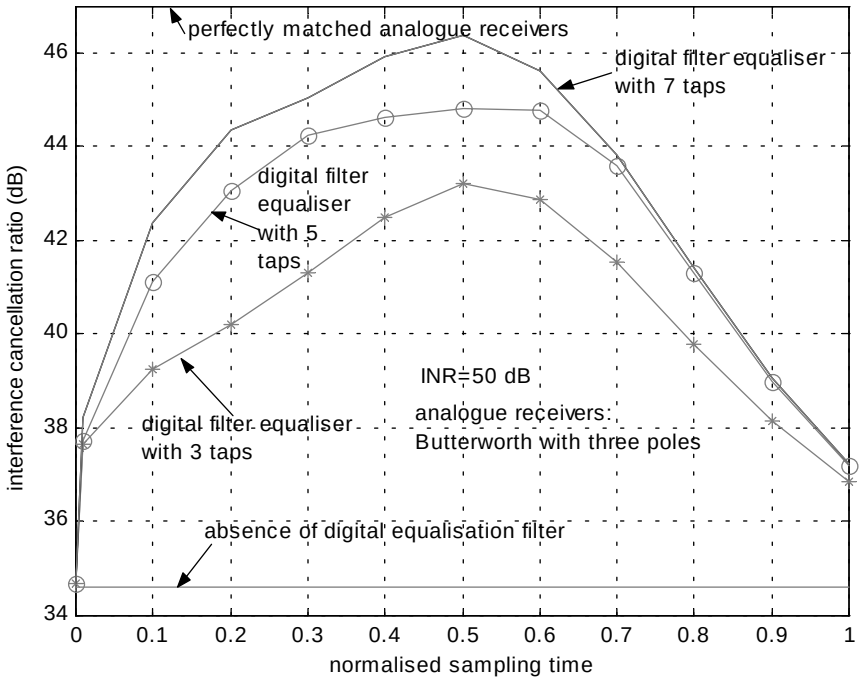

Fig. 9. ICR vs. the normalised sampling time. The analogue receivers are emulated with Butterworth filters having $M = 3$ poles; the digital equaliser has $L = 3$, 5 and 7 taps; INR = 50 dB.

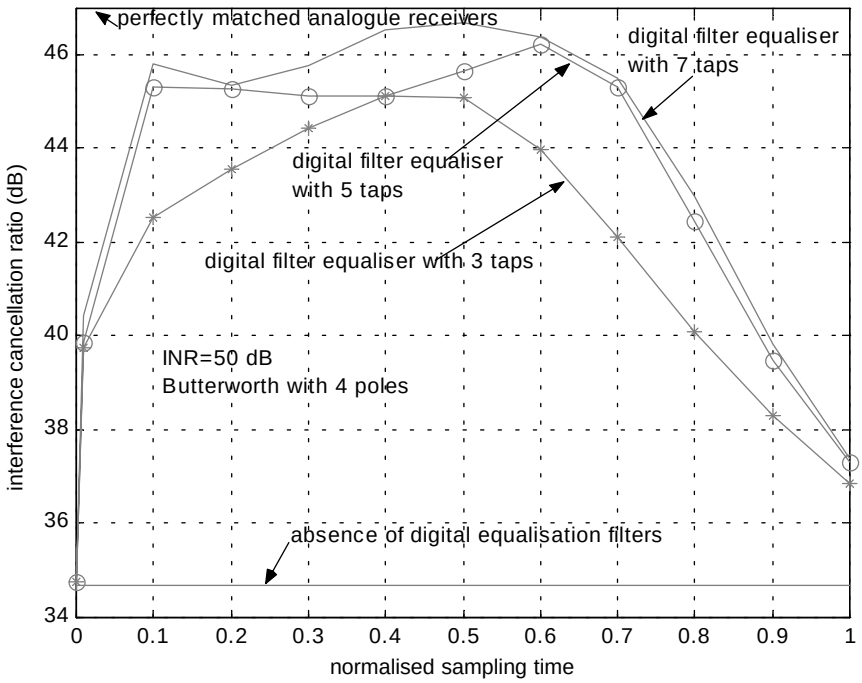

Fig. 10. ICR vs. the normalised sampling time. The analogue receivers are emulated with Butterworth filters having $M = 4$ poles; the digital equaliser has $L = 3$, 5 and 7 taps; INR = 50 dB.

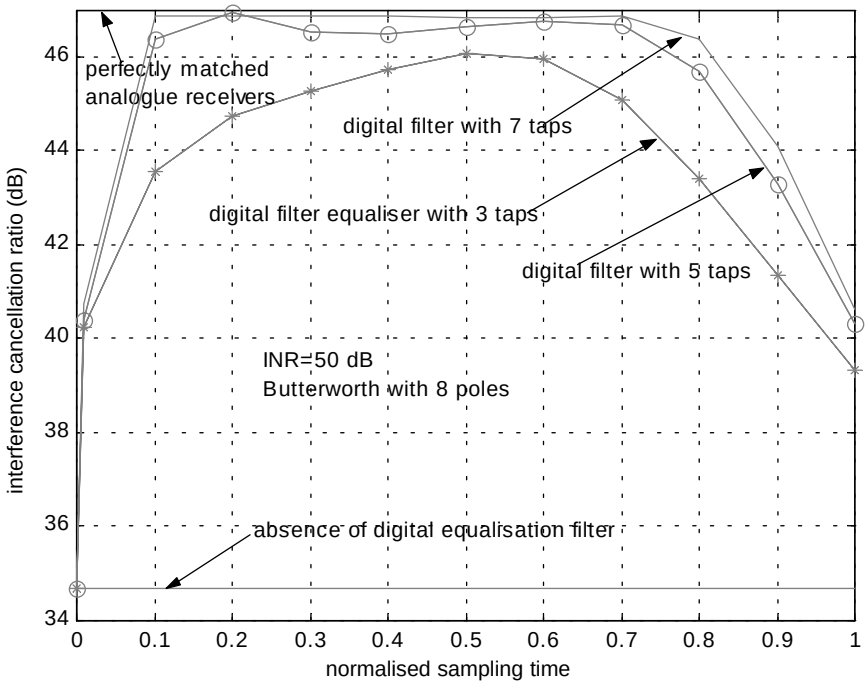

Fig. 11. ICR vs. the normalised sampling time. The analogue receivers are emulated with Butterworth filters having $M = 8$ poles; the digital equaliser has $L = 3$, 5 and 7 taps; INR = 50 dB.

2. Sampling at Nyquist rate does not give a substantial advantage of ICR whatever is the number of taps of the digital equaliser. This point deserves some further clarification. Nyquist's sampling theorem—and as a result the notion of Nyquist rate—are defined for band limited signals. The examined Butterworth filters with finite order are by no means exactly band limited. We have chosen the point of -3 dB decay of the filter amplitude to define the bandwidth: a common procedure in radar systems. This means that the amplitude has dropped to 0.5 times the maximum amplitude as per Fig. 6. It is therefore not surprising that sampling at this rate leads to a poor performance regardless of the length of the digital filter due to aliasing. Defining the bandwidth at a higher attenuation, say 30 dB, the digital equaliser would work well. In summary, we need to select a sufficiently high sampling rate to avoid the deleterious effects of the filter tails. The above analysis and the corresponding curves provide the right answer to the problem.
3. The best ICR performance are obtained when the NST is in between 0 (i.e.: $L = 1$, in practice the digital equaliser is absent) and 1 (Nyquist sampling rate). This is a consequence taken the comment 2 into account.
4. A safe value of the NST is two times the Nyquist sampling rate, i.e.: $a = 0.5$.
5. The peak of ICR is closer to the Nyquist rate, i.e.: less oversampling is needed, as the order of the Butterworth filter is increased. This is again attributable to the steeper fall off of the tails of the filter and taking into account point 2.
6. The ICR increases with the increase of the number of taps of the digital equaliser; this is due to the better approximation of the ideal transfer function (2). This result has already been stated in the past: see [2–5].
7. From Fig. 11, it appears that an almost complete recoup of the ideal ICR is obtained if the Butterworth filter has very steep fall off of the tails (i.e.: 8 poles), the number of taps of the digital FIR equaliser is $L = 8$, and the NST = 0.7, i.e.: the ADC sampling rate is only 1.4 times the Nyquist rate.

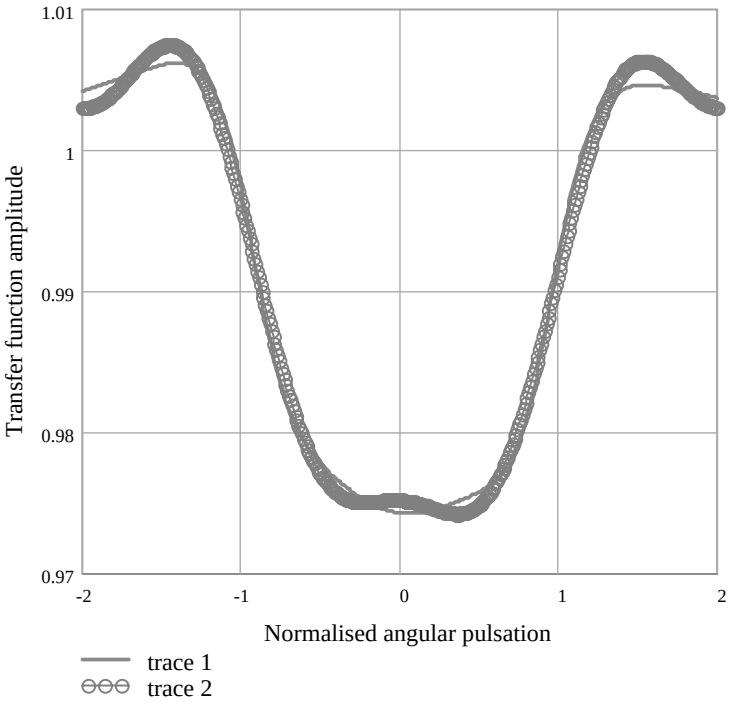

Fig. 12. Amplitude (in natural number) of the ideal (solid line) and actual (circles) digital equalisers response vs. the normalised angular pulsation. The analogue receivers are emulated with Butterworth filters having $M = 4$ poles; the digital equaliser has $L = 7$ taps; ADC normalised sampling time $a = 0.5$; INR = 50 dB.

8. All the figures show a drop of the cancellation when the sampling parameter a goes to zero. There are two reasons to have this drop:
   (i) as the sampling interval T goes to zero, while the number L of taps is kept constant, the overall duration of the equaliser goes to zero which is equivalent to the absence of equalisation; consequently the cancellation becomes the one in absence of equaliser; (ii) the frequency resolution of the equaliser is: $1/LT$; as T goes to zero the frequency resolution of the digital filter degrades to no resolution at all; consequently, the digital equaliser does not have the capability to follow the amplitude and phase variations in the frequency band of the analogue filter in the auxiliary channel. This result has also been established previously by [5,4].
9. An increase of the number of poles of the radar receivers corresponds to a more costly receiver. Thus, the trade-off between the number of receiver poles and the sampling rate of the ADC becomes a cost trade-off; this is highly dependent upon the technology available at the moment of the system design and implementation.

Figs. 12 and 13 compare the transfer functions of the digital equaliser implemented with the FIR having L taps and the ideal equaliser of Eq. (2). In particular, Fig. 12 depicts the amplitude, while Fig. 13 displays the phase of the filter transfer functions. On the horizontal axis, the normalised angular pulsation ω varies in the interval $[-1/a, 1/a]$; in our case $a = 0.5$ (i.e.: ADC sampling rate equal to two times the Nyquist rate). The analogue radar receiving channels are emulated with Butterworth filters having $M = 4$ poles (see Fig. 10); the digital equaliser has $L = 7$ taps.

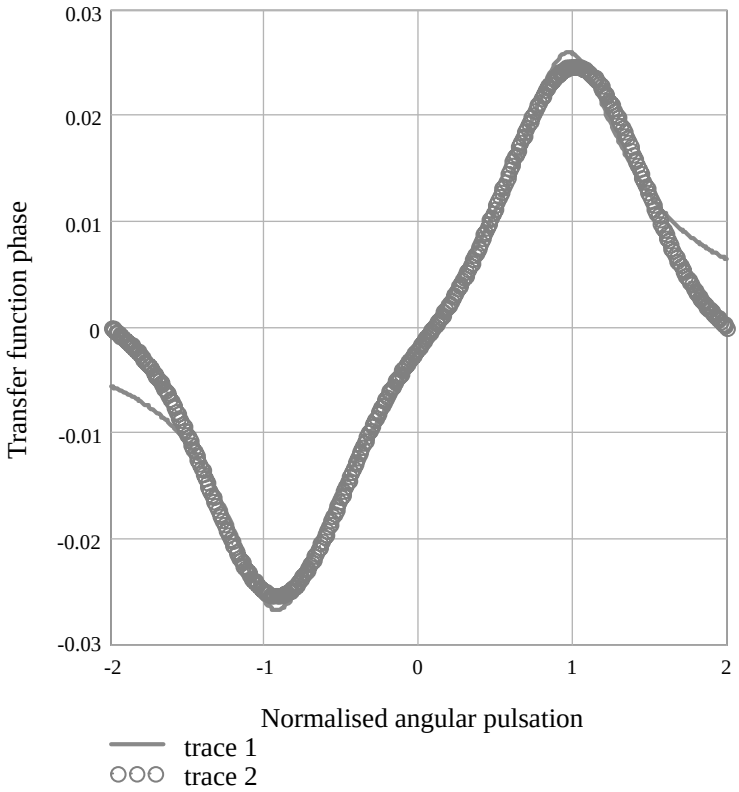

Fig. 13. The phase (in radians) of ideal (solid line) and actual (circles) digital equalisers response vs. the normalised angular pulsation ω. The analogue receivers are emulated with Butterworth filters having $M=4$ poles; the digital equaliser has $L=7$ taps; ADC normalised sampling time $a=0.5$; INR $=50$ dB.

It is seen that the digital equaliser closely follows the ideal equaliser of Eq. (2). This means that

$$H_{\mathrm{DE}}(\omega)=w_1+w_2\mathrm{e}^{\mathrm{j}\omega T}+\cdots+w_7\mathrm{e}^{\mathrm{j}\omega 6T} \tag{14}$$

with $\mathbf{w}=[w_1 w_2 \ldots w_7]^{\mathrm{T}}$ given by (3) is very close to Eq. (2), i.e.:

$$H_{\mathrm{ID}}(\omega)=\frac{\prod_{i=1}^{4}(\mathrm{j}\omega-p_i^{\mathrm{Aux}})}{\prod_{i=1}^{4}(\mathrm{j}\omega-p_i^{\mathrm{Main}})}, \tag{15}$$

where $p_i^{\mathrm{Main}},(i=1,2,3,4)$ are given by the 5th row of Table 1, while $p_i^{\mathrm{Aux}},(i=1,2,3,4)$ are the entries of the 5th row of Table 2.

5. Concluding remarks

In this paper the problem of compensating the receiver channel mismatch in an adaptive phased-array radar has been reviewed in details. This is a relevant subject which, if not properly considered, could impair the cancellation of directional interference via spatial filtering. The working principle of the digital equaliser has been discussed in detail; a comprehensive analysis has been carried out to give a method to select the typical parameters of the problems: the order of the equaliser and the ADC sampling rate.

Few more points deserve additional comments:

(i) the waveform of the calibration signal,
(ii) the power, with respect to noise, of the calibration signal,
(iii) the number of samples to estimate **R** and **r**,
(iv) the effect of the microwave couplers that inject the calibration signals, and
(v) the intermediate frequency (IF) sampling technique.

Point (i). In this paper a PRNS with enough bandwidth (say, for instance, 5 times B) has been considered. Another calibration signal could be a sequence of sinusoids suitably spaced in the calibration bandwidth $5B$. In this case, the weights of the digital equaliser can be calculated as follows:

(a) for the ith value ω_i of the angular pulsation, we measure $H_{\mathrm{M}}(\omega_i)$ and $H_{\mathrm{A}}(\omega_i)$; $i = 1, 2, \ldots, K$ being K the number of calibration sinusoids;
(b) for each ω_i calculate the response of the ideal equaliser

$$H_{\mathrm{ID}}(\omega_i) = \frac{H_{\mathrm{M}}(\omega_i)}{H_{\mathrm{A}}(\omega_i)}, \quad i = 1, 2, \ldots, K, \tag{16}$$

(c) write the K equations like this

$$H_{\mathrm{DE}}(\omega_i) \equiv w_1 + w_2 \mathrm{e}^{\mathrm{j}\omega_i T} + \cdots + w_L \mathrm{e}^{\mathrm{j}\omega_i (L-1)T} = H_{\mathrm{ID}}(\omega_i), \quad i = 1, 2, \ldots, K \tag{17}$$

with $K \geqslant L$;
(d) solve for $\mathbf{w} = [w_1 \;\; w_2 \ldots w_L]^{\mathrm{T}}$ the system of K Eq. (17), by resorting to the classical pseudo-inverse algorithm.

The preference of this Author goes to the use of the PRNS; in fact, it avoids to synthesise K (a number to determine with a suitable rationale) sinusoids of high spectral purity.

Point (ii). It is obvious that a low value of the power of the calibration signal with respect to noise will not allow a good estimation of **R** and **r** with a consequent bad reproduction of the ideal equalisation filter (2). The ICR is a monotonic increasing function of the power of the calibration signal with respect to noise. Thus, a safe criterion to select the power of the calibration signal is related to the desired ICR. For instance, if the required ICR is 47 dB, the power of the calibration signal with respect to noise should be 50 dB as it was applied in all our previous numerical examples.

Point (iii). The matrix **R** and the vector **r** (Eqs. (4) and (5), respectively), are not a priori known and have to be estimated by the data received during the learning phase. It is well known that if L is the dimension of the covariance matrix to estimate, the number of independent samples to use for the estimation should be at least 2–$3L$ (see, for instance, [2, p. 131]). Because the length of input signal (i.e.: the PRNS) during the learning phase is not strongly bounded, a safe value of 100 samples can be taken to estimate the covariance matrix with $L \cong 10$; this choice has been successfully tested by Monte Carlo simulation (detailed results not shown in this paper).

Point (iv). In Figs. 2 and 3 we have tacitly hypothesised that the microwave couplers have unity transfer function in order not to affect the calibration procedure. In reality, the couplers have their own transfer functions which in general might have very small differences from coupler to coupler. Indeed, the differences are very modest; in fact, the couplers are pieces of wave guide having the same length within very good tolerances. In conclusions, the limitations to ICR introduced by the couplers are so small that can hardly be appreciated by high-quality laboratory instruments used, for instance, to measure the correlation coefficient of signals at the output of a pair of couplers having at their input the same PRNS. It happens that the correlation coefficient is very close to one such that the corresponding ICR is much greater than the 50 dB considered in our numerical examples of Section 4. The idea to use a calibration signal in front of the antenna, thus avoiding the use of couplers, does not solve the problem; in fact, multipath effect might provide slightly different calibration signals at the channel inputs.

Point (v). It is a trend of today technology to perform the digital conversion of the received radar signal at IF (see, for instance, [2, pp. 43–48]). A remarkable advantage of the IF sampling is the absence of the

imbalance (in amplitude, phase and time) between the I and Q signal components generated by the analogue base-band receivers. This is paid by the need of an ADC with a quite high sampling rate (e.g.: four times the Nyquist sampling rate) and the need of long (hundreds of taps) digital interpolation filters to reconstruct the I and Q signals from the IF digital sequence. These interpolation filters, with properly modified weights, may also perform the equalisation of the analogue receivers. Additionally, due to the large number of taps, these filters will be designed to have sharp fall-off thus reducing the effects of the aliasing of the tails of the analogue filters of the receiving channels.

Acknowledgements

The author and his colleagues Drs. L. Timmoneri and R. Sanzullo have experimentally checked the benefits achieved, in terms of channel equalisation, by oversampling the received radar signals. Prof. F. Gini (University of Pisa) carefully read the manuscript suggesting several improvements.

Appendix A

In this section, we calculate the expression of ICR versus the amplitude and phase mismatches for a simple adaptive array radar made of a main and an auxiliary channels. The processing scheme we analyse is depicted in Fig. 14. The bold lines after the base-band conversion mean that the signal is complex valued, i.e.: it has the in phase and quadrature components.

The channels are made of proper antennas and analogue receivers. The antenna gains are $G_{\mathrm{M}}(\theta), G_{\mathrm{A}}(\theta)$, where θ is the generic angle of arrival of a wave; planar geometry is considered for simplicity. The transfer functions of the two receivers are (see also [3,5])

$$H_{\mathrm{M}}(f) = \begin{cases} H_0 \mathrm{e}^{-\mathrm{j}m_{\mathrm{M}}f}, & |f| \leqslant B/2, \\ 0, & \text{otherwise}, \end{cases} \tag{A.1}$$

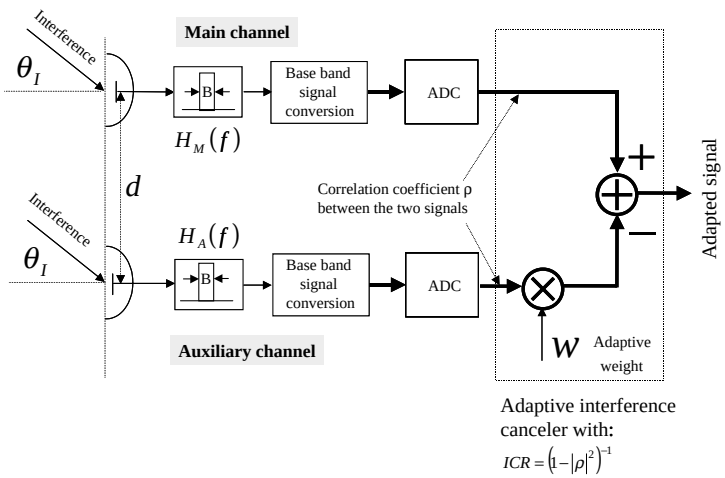

Fig. 14. Processing scheme to analyse the effect on the ICR of the receiver mismatches.

$$H_{\mathrm{A}}(f)=\begin{cases}\left[H_0-a_{\mathrm{A}}\cos\left(\dfrac{2\pi f}{B}\right)\right] & \\ \quad\times \mathrm{e}^{-\mathrm{j}(m_{\mathrm{M}}f-b\cos(2\pi f/B))}, & |f|\leqslant B/2,\\ 0, & \text{otherwise,}\end{cases} \tag{A.2}$$

where B, H_0, m_{M}, a_{A} and b are, respectively, the bandwidth of the base-band analogue receivers, the reference value of the amplitude response of the main receiver, the reference value of the phase response slope of the main receiver, the amplitude and phase mismatches of the auxiliary receiver with respect to the main receiver taken as reference.

The sinusoidal mismatch is a suitable mathematical model to perform calculations; it occurs also in practical systems. In the model above just one oscillation of the ripples in the channel bandwidth is hypothesised. In general, the oscillations may be more than one (3.5 oscillations are reported in [1, p. 305]); in this case the calculations can be done accordingly. An interference is impinging with an angle θ_{I} with respect to the normal to the array face. The correlation coefficient between the signals received by the two channels has the following expression:

$$\rho=\frac{(G_{\mathrm{M}}^{*}(\theta_{\mathrm{I}})G_{\mathrm{A}}(\theta_{\mathrm{I}})\mathrm{e}^{\mathrm{j}2\pi d\sin\theta_{\mathrm{I}}/\lambda_0}/B)\int_{-0.5B}^{0.5B}[1-(a_{\mathrm{A}}/H_0)\cos(2\pi(f/B))]\mathrm{e}^{\mathrm{j}[2\pi(d\sin\theta_{\mathrm{I}}/c)f+b\cos(2\pi(f/B))]}\,\mathrm{d}f}{\sqrt{(|G_{\mathrm{M}}(\theta_{\mathrm{I}})|^2+1/\mathrm{INR})(|G_{\mathrm{A}}(\theta_{\mathrm{I}})|^2+1/\mathrm{INR})(1+0.5(a_{\mathrm{A}}/H_0)^2)}}, \tag{A.3}$$

where $d, \lambda_0, \theta_{\mathrm{I}}$, and $\mathrm{INR}=P_{\mathrm{I}}/P_{\mathrm{N}}$ are, respectively, the distance between the phase centres of the main and auxiliary antennas, the wave length of the carrier, the IDoA, and the interference-to-noise power ratio.

From [2, p. 101], it is known that

$$\mathrm{ICR}=\frac{1}{1-|\rho|^2}. \tag{A.4}$$

Substituting (A.3) into (A.4) gives the expression of the ICR as a function of many parameters. For our purposes, we may take $\theta_{\mathrm{I}}=0^{\circ}$ which corresponds to the highest ICR value. Additionally, we set $G_{\mathrm{M}}(\theta)=G_{\mathrm{A}}(\theta)=1$; in fact, these terms are not relevant for the analysis of mismatching limitations. The previous expression (A.4) becomes

$$\mathrm{ICR}=\frac{1}{1-|(1/B)\int_{-0.5B}^{0.5B}[1-a_{\mathrm{n}}\cos(2\pi(f/B))]\mathrm{e}^{\mathrm{j}[b\cos(2\pi(f/B))]}\,\mathrm{d}f/(1+1/\mathrm{INR})\sqrt{(1+0.5a_{\mathrm{n}}^2)}|^2}, \tag{A.5}$$

where $a_{\mathrm{n}}=a_{\mathrm{A}}/H_0$. Setting $\mathrm{INR}\to\infty$ and $b=0$, we obtain $\mathrm{ICR}=1+2/a_{\mathrm{n}}^2\cong 2/a_{\mathrm{n}}^2$; this result is equal to the one mentioned in Section 2 for a sinusoidal ripple of the amplitude with a frequency different from one.

Appendix B

Table 1 provides the numerical values of the poles for ideal Butterworth filters of order $M=1$, 2, 3, 4 and 8 that are used in the receiver of the main channel for several study cases; these values come from Eq. (7) in the text.

The numerical values of the poles for the mismatched Butterworth filters of order $M=1$, 2, 3, 4 and 8 are in Table 2; these are used in the receivers of the auxiliary channels.

Appendix C

We wish to prove Eq. (13). Consider the output signal v of Fig. 4

$$v=x_{\mathrm{M}}-\mathbf{w}^{\mathrm{T}}\mathbf{x}. \tag{C.1}$$

The power of this residue signal is

$$E\{|v|^2\} = E\{|x_M|^2\} - E\{|\mathbf{w}^T\mathbf{x}|^2\} = E\{|x_M|^2\} - \mathbf{w}^H\mathbf{R}\mathbf{w} \tag{C.2}$$

by substituting (3) in (C.2), we obtain

$$E\{|v|^2\} = E\{|x_M|^2\} - \mathbf{r}^H\mathbf{R}^{-1}\mathbf{r}. \tag{C.3}$$

Thus the ICR can be written as follows:

$$\begin{aligned}\mathrm{ICR} &= \frac{P_I + P_N}{E\{|v|^2\}} = \frac{P_I + P_N}{E\{|x_M|^2\} - \mathbf{r}^H\mathbf{R}^{-1}\mathbf{r}} = \frac{P_I + P_N}{P_I + P_N - \mathbf{r}^H\mathbf{R}^{-1}\mathbf{r}} \\ &= \frac{1}{1 - \mathbf{r}^H\mathbf{R}^{-1}\mathbf{r}/(P_I + P_N)} = \frac{1}{1 - \mathbf{r}^H\mathbf{R}^{-1}\mathbf{r}/P_I(1 + 1/\mathrm{INR})}\end{aligned} \tag{C.4}$$

Eq. (13) immediately follows by taking $P_I = 1$; this is a consequence of $\int_{-\infty}^{\infty} |H_M(\omega)|^2 \, d\omega = 1$, an assumption already made in writing Eq. (8).

References

[1] B.D. Carlson, L.M. Goodman, J. Austin, M.W. Gantz, L.O. Upton, An ultralow-sidelobe adaptive array antenna, Lincoln Lab. J. 3 (2) (Summer 1990) 291–310.
[2] A. Farina, Antenna Based Signal Processing Techniques for Radar Systems, Artech House, Inc, Norwood, MA, USA, 1992.
[3] A. Farina, A. Protopapa, Channel mismatching in sidelobe canceler: limitations and remedies, Chin. J. Systems Electron. 3 (3) (1992) 23–43.
[4] K. Gerlach, The effects of the IF band pass mismatch errors on adaptive cancellation, IEEE Trans. Aerospace Electron. Systems AES-26 (3) (May 1990) 455–468.
[5] R.A. Monzingo, T.W. Miller, Introduction to Adaptive Arrays, Wiley, New York, 1980.
[6] U. Nickel, On the influence of channel errors on array signal processing methods, Int. J. Electron. Commun. (AEÜ) 47 (4) (1993) 209–219.
[7] R. Nitzberg, Adaptive Signal Processing for Radar, Artech House, Norwood, MA, 1992.
[8] J. Ward, Space-time adaptive processing for airborne radar, TR. 1015, MIT Lincoln Laboratory, 13 December 1994.